Differentiation of Nonarteritic Anterior Ischemic Optic Neuropathy from Normal Tension Glaucoma by Comparison of the Lamina Cribrosa

Jeong-Ah Kim,[1] Eun Ji Lee,[2] Tae-Woo Kim,[2] Hyunjoong Kim,[3] Michaël J.A. Girard,[4,5] Jean Martial Mari,[6] Hee Kyung Yang,[2] and Jeong-Min Hwang[2]

[1]Department of Ophthalmology, Kangwon National University School of Medicine, Chuncheon, South Korea
[2]Department of Ophthalmology, Seoul National University College of Medicine, Seoul National University Bundang Hospital, Seongnam, South Korea
[3]Department of Applied Statistics, Yonsei University, Seoul, South Korea
[4]Department of Biomedical Engineering, National University of Singapore, Singapore, Singapore
[5]Singapore Eye Research Institute, Singapore National Eye Centre, Singapore, Singapore
[6]GePaSud, Université de la Polynésie Française, Tahiti, French Polynesia

Correspondence: Eun Ji Lee, Department of Ophthalmology, Seoul National University Bundang Hospital, 82, Gumi-ro, 173 Beon-gil, Bundang-gu, Seongnam-si, Gyeonggi-do 13620, South Korea; opticdisc@gmail.com.

Received: February 2, 2020
Accepted: May 27, 2020
Published: July 15, 2020

Citation: Kim J-A, Lee EJ, Kim T-W, et al. Differentiation of nonarteritic anterior ischemic optic neuropathy from normal tension glaucoma by comparison of the lamina cribrosa. *Invest Ophthalmol Vis Sci.* 2020;61(8):21. https://doi.org/10.1167/iovs.61.8.21

Purpose. To compare lamina cribrosa (LC) morphology between eyes with nonarteritic anterior ischemic optic neuropathy (NAION) and eyes with normal tension glaucoma (NTG) in the Korean population.

Methods. This retrospective study included 48 eyes with NAION, 48 eyes with NTG, and 48 healthy control eyes matched by age, intraocular pressure, axial length, and optic disc area. Eyes with NAION and NTG were also matched by retinal nerve fiber layer (RNFL) thickness in the affected sector. Optic nerve heads were scanned using enhanced depth imaging spectral-domain optical coherence tomography. LC depth (LCD) and the LC curvature index (LCCI) were measured at seven locations spaced equidistantly across the vertical optic disc diameter. LCD and the LCCI were compared in the three groups.

Results. RNFL thicknesses of the matched affected sectors did not differ between the NAION and NTG groups ($P = 0.347$). LCD and the LCCI were significantly larger in the NTG group than in the NAION and healthy control groups at all seven planes ($P < 0.001$ each), but were comparable in the NAION and healthy control groups. The LCCI was larger in the affected than in the unaffected sector of NTG eyes ($P = 0.010$) but did not differ in NAION eyes ($P = 1.000$). LCD did not differ between affected and unaffected sectors in either NAION ($P = 0.600$) or NTG ($P = 0.098$) eyes.

Conclusions. LC morphology differed in eyes with NAION and NTG, despite a similar degree of RNFL damage. Evaluation of LC morphology may help to understand the distinctive pathophysiology of NAION and to differentiate NAION from NTG eyes.

Keywords: nonarteritic anterior ischemic optic neuropathy, normal tension glaucoma, lamina cribrosa, optic nerve head, optic neuropathy

Nonarteritic anterior ischemic optic neuropathy (NAION) is the most common type of acute ischemic optic neuropathy caused by the transient nonperfusion or hypoperfusion of the optic nerve head (ONH) circulation in middle-aged and elderly individuals.[1] In the active phase, NAION typically manifests as a sudden painless visual loss or optic disc edema with hemorrhages on the disc margins, eventually resulting in optic disc pallor and adjacent retinal nerve fiber layer (RNFL) defects with corresponding visual field (VF) damage at the affected sector. Because the blood vessels supplying the superior and inferior sectors of the ONH are not reconnected distally, the pattern of RNFL defects and VF damage may sometimes mimic glaucomatous optic neuropathy (GON),[2–4] especially normal tension glaucoma (NTG). Differentiating NAION from GON is even more challenging when either disease is not accompanied by a typical optic disc appearance or when the change in the optic disc appearance is subtle. In addition, the history of the visual symptom is not helpful in differential diagnosis in some patients with unilateral disease, as they are often unaware of visual loss.[5]

In glaucoma, deformation of the ONH tissue,[6–9] such as excavation of the scleral canal and/or posterior bowing of the lamina cribrosa (LC), is an important pathogenic event in the development of GON. Even in NTG, the LC was found to be more deformed than in fellow healthy eyes,[10] indicating that LC remodeling may be involved in the pathogenesis of NTG. LC deformation together with thinner prelaminar tissue in NTG may attribute to acquired excavation (i.e., cupping) of the ONH, which is a distinctive feature distinguished from

that observed in NAION (i.e., pallor). Such a difference in the deep ONH morphology may explain the different pathogenesis of NTG and NAION.

Studies evaluating the LC in NAION have mainly assessed LC deformation by measuring the level of anterior LC surface relative to the level of the Bruch's membrane opening (i.e., LC depth).[11,12] However, such measurement is affected by choroid thickness, which has been reported to be thicker in eyes with NAION than in healthy eyes[13] and has considerable inter-individual[14] and intra-individual regional variability.[15] The present study, therefore, compared LC morphology in terms of LC depth (LCD) and curvature (LC curvature index, LCCI), in eyes with NAION and treatment-naïve NTG. We hoped that determination of the differences in LC morphology could provide further insight into the pathophysiology of NAION compared to that of NTG.

Methods

This was a retrospective cross-sectional study that included Korean subjects diagnosed with either NAION or NTG and healthy control subjects. Patients with NAION were selected from among individuals who visited Seoul National University Bundang Hospital (SNUBH) from January 2012 to December 2018. Patients with treatment naïve NTG and healthy control participants were selected from individuals enrolled in the Investigating Glaucoma Progression Study, an ongoing prospective investigation of glaucoma and normal controls at the SNUBH Glaucoma Clinic. The study protocol was approved by the institutional review board of SNUBH and was performed in accordance with the tenets of the Declaration of Helsinki.

Subjects

All subjects underwent comprehensive ophthalmic examinations, including best-corrected visual acuity, Goldmann applanation tonometry, refraction tests, slit-lamp biomicroscopy, gonioscopy, stereodisc photography, and red-free fundus photography (EOS D60 digital camera; Canon Inc., Tokyo, Japan). Other examinations included measurements of corneal curvature (KR-1800 Auto Kerato-Refractometer; Topcon, Tokyo, Japan), central corneal thickness (Orbscan II; Bausch & Lomb, Rochester, NY, USA), and axial length (AXL) (IOLMaster V.5; Carl Zeiss Meditec, Jena, Germany); spectral-domain optical coherence tomography (SD-OCT) scanning of the circumpapillary RNFL and ONH in the enhanced depth imaging (EDI) mode (Spectralis; Heidelberg Engineering, Heidelberg, Germany); and standard automated perimetry (Humphrey Field Analyzer II 750 and 24-2 Swedish interactive threshold algorithm; Carl Zeiss Meditec).

The NAION group included subjects diagnosed at least 6 months prior to study entry. NAION diagnosis was based on the sudden, painless loss of visual acuity (VA) without history of glaucoma or retinal diseases, optic disc edema with or without superficial hemorrhages at the optic disc border and adjacent retina on fundus ophthalmoscopy, or VF defects consistent with NAION and with spontaneous resolution of optic disc edema within 2 to 3 months. Subjects were excluded if they showed symptoms or signs suggesting arteritic ischemic optic neuropathy or giant cell arteritis, such as jaw claudication, anorexia, unintended weight loss, and elevated erythrocyte sedimentation rate or reactive protein C levels. Subjects were also excluded if they had been diagnosed with glaucoma, had intraocular pressure (IOP) >21 mm Hg in either eye, or if the contralateral eye had features suspicious of or consistent with glaucoma.

NTG diagnosis was based on the presence of glaucomatous optic nerve damage (i.e., notching, neuroretinal rim thinning, and/or RNFL defects) with corresponding VF loss, open angle on gonioscopy, and IOP $\leq$ 21 mm Hg over multiple measurements during office hours (9 AM to 5 PM). A glaucomatous VF defect was defined as (1) a VF outside normal limits on the glaucoma hemifield test; (2) three abnormal points, each with a <5% probability (P) of being normal and one point with $P < 1\%$ by pattern deviation; or (3) a pattern standard deviation with $P < 5\%$ if the VF was otherwise normal, as confirmed in two consecutive tests. The VF results were deemed reliable when fixation losses were <20% and the false-positive and false-negative rates were each <25%. Moreover, subjects with NTG were required to have no history of IOP-lowering treatment. Healthy eyes were defined as those with no history of ocular symptoms, disease, or intraocular surgery except for uncomplicated cataract extraction. Normal eyes also had an IOP of $\leq$21 mm Hg, an absence of glaucomatous optic disc appearance, and no VF defect.

In each patient with NAION, either the superotemporal or inferotemporal sector of the eye affected by disease was selected as the sector of interest. If both sectors were affected, the more severely affected sector was selected based on RNFL thickness. NTG patients and healthy controls were selected by matching them 1:1:1 with NAION patients by age (within 5 years), IOP (within 1 mm Hg), AXL (within 1 mm), and optic disc area (ODA; within 1 mm^2). NAION and NTG patients were also matched by RNFL thickness in the sector of interest (within 10 µm); the sector of interest in the healthy controls was the sector selected in the matched NAION patients. The ODA was measured by two experienced investigators (J.-A.K. and E.J.L.), who were masked to patient clinical information, using the built-in manual caliper tool designed to calculate the area of fundus images in Heidelberg Eye Explorer (software version 1.10.4.0, Heidelberg Engineering), a viewer program provided with the Spectralis OCT device. The final ODA was defined as the average of the two measurements, one made by each investigator.

Patients were excluded who had a spherical equivalent < –6.0 D or > +3.0 D; a cylinder correction < –3.0 D or > +3.0 D; a tilted disc (i.e., tilt ratio > 1.3 of the longest to the shortest diameter of the optic disc);[16,17] or a torted disc (i.e., a torsion angle deviation of the long axis of the optic disc from the vertical meridian > 15°).[17,18] Also excluded were patients with optic disc pallor from concomitant retinal diseases, such as diabetic retinopathy, retinal venous obstruction, retinal arterial obstruction, or retinitis pigmentosa, as well as those who had previously undergone unilateral cataract surgery to exclude pseudophakic pallor. The ovality index of the optic disc was defined as the ratio of the longest to the shortest disc diameters by the clinical optic disc margins on color photographs using ImageJ (National Institutes of Health, Bethesda, MD, USA). Eyes were also excluded if a good-quality image (i.e., quality score > 15) could not be obtained in more than five sections. If the quality score did not reach 15, the image-acquisition process automatically stopped or images of the respective sections were not obtained. LCD and the LCCI were measured only on acceptable scans with good-quality images that allowed clear delineation of the anterior borders of the LC within the

Investigative Ophthalmology & Visual Science

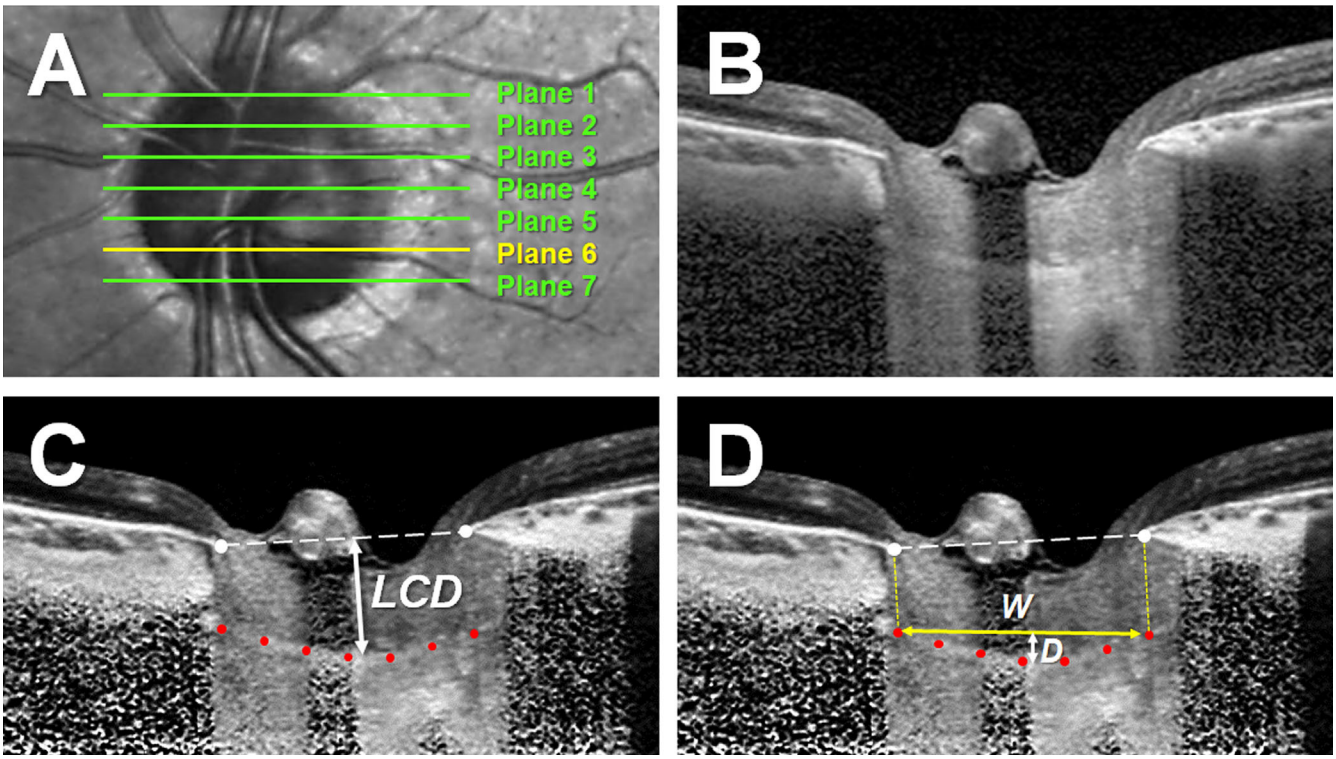

Figure 1. Measurements of LCD and the LCCI. (**A**) Infrared fundus image of an optic nerve head with lines indicating the locations at which the seven B-scan images were obtained. (**B**) B-scan image obtained at plane 5 in **A**. (**C**, **D**) Same B-scan images as in **B**, postprocessed by adaptive compensation. (**C**) LCD was defined as the maximum vertical distance from the BMO reference line (*dashed line*) to the anterior LC surface (*double-headed arrow*). (**D**) The LCCI was measured by dividing the LC curve depth (*D*) within the BMO by the width of the anterior LC surface reference line (*W*) and then multiplying the ratio by 100.

range of the width of Bruch's membrane opening (BMO). IOP was measured on the same day that ONH was imaged by SD-OCT using the EDI technique.

EDI-OCT of the Optic Nerve Head and Adaptive Compensation

The LC configuration was assessed on horizontal B-scan images obtained using the EDI technique of the SD-OCT system at the high-speed setting.[14] Prior to disc scanning, the corneal curvature of each eye was entered into the Spectralis OCT system to avoid potential magnification errors. The optic disc was imaged through undilated pupils using a rectangle subtending 10° × 15° of the optic disc. This rectangle was scanned with approximately 75 B-scan section images that were separated by 30 to 34 µm, with the distance between the scan lines determined automatically. Approximately 42 SD-OCT frames were obtained for each section. This protocol provided the best trade-off between image quality and patient cooperation.[19] To enhance the visibility of the anterior LC surface, all disc scan images were postprocessed using adaptive compensation.[20–22]

Measurement of LC Depth and Curvature

The LCD and LCCI were measured at seven locations equidistant across the vertical optic disc diameter on postprocessed horizontal B-scan images. These seven B-scan lines were defined as planes 1 to 7 (superior to inferior regions) (Fig. 1A). In this model, plane 4 corresponded to the mid-horizontal plane, and planes 2 and 6 corresponded to the superior and inferior midperiphery planes, respectively.

Because a bowtie-shaped central ridge is present at or near the mid-horizontal LC,[23] the LC usually has a W shape in vertical scans while varying in radial scans along the meridians. Therefore, it is difficult to assess the LC configuration using a simple parameter, such as the LCCI, in vertical or oblique scans. In contrast, LC has a relatively regular configuration in the horizontal plane, having a flat or U-shaped appearance differing in regional steepness.[24–26] Therefore, LCD and the LCCI were assessed on horizontal scans.

The LCD was defined as the distance between the level of the BMO and the maximally depressed point of the anterior LC surface. A line connecting the temporal and nasal BMO points was drawn on each B-scan image, and the LCD was measured perpendicular to this line toward the maximally depressed LC point (Fig. 1B). The distance between the temporal and nasal BMO points was defined as the BMO width.

The LC curvature was assessed by measuring the LCCI. The method used to calculate the LCCI has been described previously.[25,27–30] In brief, the LCCI was determined by measuring the width of the LC curve reference line (LCCW) and the LC curve depth (LCCD). The LCCW was defined as the width of the line connecting the two points on the anterior LC surface that met the lines drawn from each Bruch's membrane termination point perpendicular to the line connecting these BMO points. The maximum depth from the LC curve reference line to the anterior LC surface

Investigative Ophthalmology & Visual Science

Table 1. Demographic Characteristics of the Study Subjects

Variables	Groups (A) NAION Eyes ($N = 48$)	(B) NTG Eyes ($N = 48$)	(C) Healthy Eyes ($N = 48$)	P^*	Post Hoc†
Age at diagnosis (y)	60.8 ± 9.1	60.3 ± 9.2	61.7 ± 10.0	0.773	—
Female gender, *n* (%)	20 (41.67)	23 (47.92)	28 (58.33)	0.256	—
Diabetes mellitus, *n* (%)	10 (20.83)	5 (10.42)	9 (18.75)	0.350	—
Hypertension, *n* (%)	25 (52.08)	15 (31.25)	14 (29.17)	**0.037**	**A > B, C**
IOP at OCT scan (mm Hg), mean ± SD	12.1 ± 2.8	12.5 ± 2.2	11.9 ± 2.0	0.442	—
Refractive error (D), mean ± SD	–0.11 ± 1.98	–0.68 ± 1.80	0.02 ± 1.32	0.115	—
Central corneal thickness (μm), mean ± SD	545.5 ± 24.7	546.4 ± 31.7	548.7 ± 27.8	0.853	—
Axial length (mm), mean ± SD	23.42 ± 0.88	23.57 ± 0.82	23.52 ± 0.82	0.700	—
Involved hemifield, *n* (%)					—
Superior	44 (91.67)	44 (91.67)	—	—	—
Inferior	4 (8.33)	4 (8.33)	—	—	—
RNFL thickness of the sector of interest‡ (μm), mean ± SD	68.0 ± 20.9	66.5 ± 18.5	135.5 ± 12.9	**<0.001**	**C > A, B**
Visual field mean deviation (dB), mean ± SD	–11.64 ± 8.87	–10.16 ± 6.23	-0.81 ± 1.47	**<0.001**	**C > A, B**
Visual field pattern standard deviation (dB), mean ± SD	8.90 ± 4.47	8.56 ± 4.47	1.77 ± 0.70	**<0.001**	**C > A, B**
Optic disc area (mm^2), mean ± SD	2.14 ± 0.33	2.15 ± 0.29	2.12 ± 0.34	0.903	—
Average BMO width (μm), mean ± SD	1358.9 ± 125.3	1403.9 ± 149.2	1396.1 ± 136.7	0.233	—

Factors with statistical significance are shown in bold.
* χ^2 tests for categorical variables and one-way ANOVA with Bonferroni's post hoc analysis for continuous variables.
† χ^2 tests for categorical variables and Student's *t*-test for continuous variables.
‡ Determined based on the more severely affected sector.

was defined as the LCCD (Fig. 1C). The LCCI was calculated as (LCCD/LCCW) × 100. Because the curvature is normalized relative to LC width, it describes the shape of the LC independent of the actual size of the ONH. Only the LC within the BMO was considered because the LC was often not clearly visible outside the BMO. In eyes with LC defects, the LCCI and LCD were measured using a presumed anterior LC surface that best fit the curvature of the remaining part of the LC or excluded the area of the LC defect. The LC defect was defined as an anterior laminar surface irregularity violating the smooth curvilinear U- or W- shaped contour with a diameter greater than 100 μm and a depth greater than 30 μm in cross-sectional EDI-OCT images.[31–32]

Measurements were made by two experienced observers (J.-A.K. and E.J.L.), masked to the clinical information of participants, using a manual caliper tool in Amira 5.2.2 software (Visage Imaging, Berlin, Germany). If the anterior LC surface was not visualized clearly, measurements were made on an adjacent horizontal EDI-OCT scan, located 30 to 34 μm from the original scan. If the anterior LC surface could not be visualized, even on the adjacent scans, the eye was excluded. The average LCD and LCCI were defined as the means of the measurements taken at seven points along the LC. The mean LCD and LCCI in the superior- and inferior-most two planes were defined as those in the superior and inferior sectors, respectively, and were used for determining the values in the sector of interest. The mean of the measurements made by the two observers was used for analysis.

Statistical Analysis

Data were expressed as mean ± standard deviation (SD) except where otherwise indicated. The inter-observer agreement for measuring LCD and the LCCI was evaluated by calculating the 95% Bland–Altman limits of agreement. Independent comparisons among the three groups were performed using Pearson's χ^2 tests for categorical variables. Comparisons of the LCD and LCCI between the groups were performed using one-way ANOVA based on the mean squared error that was calculated over all regions to account for spatial covariance between regions within the same eye. Bonferroni's post hoc analysis was used to assess inter-group differences. The Wilcoxon signed-rank test or the paired *t*-test was performed for intra-individual comparison. For all analyses, parametric or nonparametric tests were utilized based on the normality. Comparison of the LCD and LCCI among the groups was performed using the rpart package in R 3.6.3 (The R Foundation, Vienna, Austria; http://www.rproject.org). Other statistical analyses were performed using SPSS Statistics 22.0 software (IBM, Armonk, NY, USA). $P < 0.05$ was considered statistically significant.

Results

Of the 53 NAION patients originally enrolled, five were excluded because of the poor quality of their EDI B-scan images, which did not allow clear visualization of the anterior LC surface in EDI B-scan images. Forty-eight NTG patients, matched in age, IOP, AXL, ODA, and RNFL thickness to the 48 NAION patients, and 48 healthy controls, matched in age, IOP, AXL, and ODA, were selected. The clinical characteristics of these three groups of study participants are shown in Table 1. There were no inter-group differences in age, sex, prevalence of diabetes mellitus, spherical equivalent, IOP at OCT scanning, central corneal thickness, AXL, ODA, or average BMO widths ($P > 0.2$ each). The prevalence of systemic hypertension was significantly higher in NAION patients than in NTG patients and healthy controls ($P = 0.037$).

Both the superior and inferior hemi-ONHs were affected in 32 of the 48 eyes with NAION, with the superior hemi-ONH being more severely affected in 31 of these eyes. A single hemi-ONH was affected in the remaining 16 eyes,

Investigative Ophthalmology & Visual Science

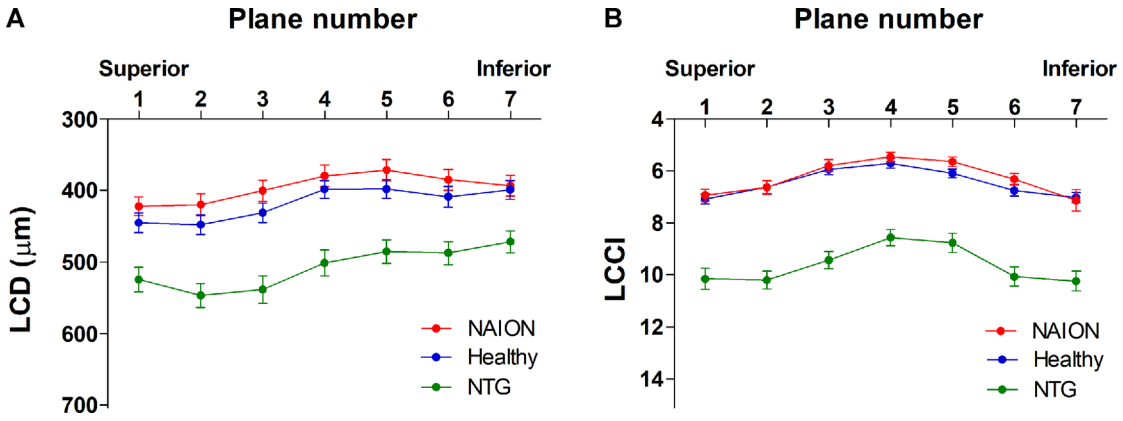

Figure 2. LCD (**A**) and the LCCI (**B**) in seven horizontal planes of EDI SD-OCT scans of NAION, NTG, and healthy eyes. Planes 1 and 7 correspond to the superior- and inferior-most planes, respectively. The LCDs and LCCIs were both larger in all seven planes of NTG compared to the NAION and healthy eyes ($P < 0.001$ each), but did not differ in the latter two groups ($P > 0.10$). Note that LCD is largest in the superior planes, gradually decreasing when moving to the inferior planes, whereas the LCCI increases similarly in both directions from the mid-horizontal plane in all three groups.

with the superior hemi-ONH being affected in 13 eyes and the inferior hemi-ONH in three. Thus, the superotemporal and inferotemporal sectors were the sectors of interest in the eyes of 44 and four patients, respectively. Accordingly, patients with NTG were selected by matching their superotemporal and inferotemporal RNFL thicknesses in 44 and four eyes, respectively. Both hemi-ONHs were affected in 26 NTG patients, with all 26 showing more severe damage in the superior sector. The superior hemi-ONH alone was affected in 18 patients and the inferior hemi-ONH in four patients. RNFL thickness in the matched sectors (i.e., sectors of interest) did not differ significantly in eyes with NAION and NTG (68.0 ± 20.9 μm vs. 66.5 ± 18.5 μm; $P = 0.347$) (Table 1).

Comparison of LCD and the LCCI

The 95% Bland–Altman limits of agreement of the measurements made by the two glaucoma specialists were –20.79 to 22.79 μm for LCD and –0.77 to 0.83 for the LCCI. In all three groups of eyes, LCD was largest in the superior planes, gradually decreasing when moving to the inferior region (Fig. 2A). In contrast, the LCCI increased similarly with distance from the mid-horizontal plane in both the superior and inferior directions (Fig. 2B). The average LCD and LCCI were significantly greater in NTG eyes than in either NAION or healthy control eyes ($P < 0.001$ each), but did not differ significantly in NAION and healthy eyes (Table 2, Fig. 2). Intra-individual comparisons in the eyes that showed involvement of a single hemi-ONH found that the LCCI was larger in the affected than in the unaffected sector of NTG eyes ($n = 22$, $P = 0.010$) but did not differ in NAION eyes ($n = 16$, $P = 1.000$) and healthy control eyes ($n = 48$, $P = 0.745$) (Table 3). LCD did not differ between affected and unaffected sectors in either NAION or NTG eyes but was larger in the superior than in the inferior sector of healthy control eyes.

Representative Case

Figure 3 shows that LCD and the LCCI in the affected sector were greater in an eye with NTG than in an eye with NAION, despite their age, IOP, AXL, RNFL thickness, and VF index being similar. Interestingly, the LCCI was greater in the affected than in the unaffected sector of the NTG eye, but this regional difference was not observed in the NAION eye.

Discussion

The present study demonstrated that LC morphology, as assessed by LCD and the LCCI, differed significantly between groups of patients with NAION and NTG, despite their having similar IOPs and similar RNFL thicknesses. To our knowledge, the present study is the first to compare LC morphology in the eyes of patients with NAION and treatment-naïve NTG.

The value of this study lies in its data, which show definitively that the LCCI and LCD are significantly larger in NTG versus NAION eyes with identical IOPs and axonal damage. This suggests that LC and ONH morphology are fundamentally different in optic neuropathies in which VF loss and RNFL thinning are very similar, in addition to strongly suggesting that the pathophysiology of these two conditions are very different. In this regard, the study is much more powerful because the patients were so carefully matched in their ocular and demographic parameters.

NAION is an acute ischemic optic neuropathy caused by the transient nonperfusion or hypoperfusion of the ONH. Because the vascular system supplying the ONH is separated into superior and inferior halves,[33] which are not reconnected distally, eyes affected by NAION usually show an RNFL thinning selective to the superior or inferior hemiretina, with altitudinal VF defect.[2,3] On the other hand, glaucoma is caused by mechanical stress on the ONH, in which the LC has been considered the principal site of axonal injury of retinal ganglion cells.[34] LC deformation is thought to promote axonal damage by blocking axonal transport, reducing the diffusion of nutrients from the laminar capillaries to the adjacent axons,[6] or through connective tissue remodeling.[35–37] LC deformation was shown to be greater in glaucomatous than in fellow healthy eyes in patients with unilateral NTG, despite the IOPs of the glaucomatous eyes being within the normal range,[10] indicating that

Table 2. Comparison of LCD and the LCCI in the Three Groups

Variables	Groups (A) NAION Eyes (n = 48)	(B) NTG Eyes (n = 48)	(C) Healthy Eyes (n = 48)	P^*	Post Hoc
LCD					
1	422.2 ± 90.5	522.4 ± 118.4	445.1 ± 96.1	**<0.001**	**B > A, C**
2	420.1 ± 106.7	544.5 ± 114.0	447.5 ± 94.3	**<0.001**	**B > A, C**
3	400.4 ± 103.5	536.1 ± 129.7	431.2 ± 94.0	**<0.001**	**B > A, C**
4	379.7 ± 105.7	499.5 ± 123.4	398.4 ± 87.0	**<0.001**	**B > A, C**
5	371.4 ± 104.1	483.5 ± 111.2	397.9 ± 91.1	**<0.001**	**B > A, C**
6	385.1 ± 102.3	485.6 ± 111.1	408.9 ± 100.2	**<0.001**	**B > A, C**
7	393.5 ± 100.1	470.3 ± 103.9	399.0 ± 90.9	**0.004**	**B > A, C**
Average	396.0 ± 95.7	506.0 ± 110.8	418.3 ± 85.7	**<0.001**	**B > A, C**
Sector of interest†	415.5 ± 92.65	524.3 ± 112.3	446.3 ± 93.67	**<0.001**	**B > A, C**
LCCI					
1	6.94 ± 1.59	10.09 ± 2.78	7.08 ± 1.38	**<0.001**	**B > A, C**
2	6.64 ± 1.74	10.14 ± 2.36	6.62 ± 1.62	**<0.001**	**B > A, C**
3	5.80 ± 1.60	9.38 ± 2.25	5.95 ± 1.31	**<0.001**	**B > A, C**
4	5.46 ± 1.26	8.52 ± 2.16	5.71 ± 1.22	**<0.001**	**B > A, C**
5	5.65 ± 1.30	8.72 ± 2.51	6.10 ± 1.21	**<0.001**	**B > A, C**
6	6.32 ± 1.43	10.01 ± 2.50	6.75 ± 1.39	**<0.001**	**B > A, C**
7	7.14 ± 2.85	10.18 ± 2.61	7.03 ± 1.38	**<0.001**	**B > A, C**
Average	6.28 ± 1.89	9.58 ± 1.87	6.46 ± 0.95	**<0.001**	**B > A, C**
Sector of interest†	6.75 ± 1.46	9.46 ± 2.29	6.85 ± 1.29	**<0.001**	**B > A, C**

Data are mean ± SD. Factors with statistical significance are shown in bold.

* One-way ANOVA based on the mean squared error, which was calculated over all regions to account for spatial covariance between regions within the same eye. Bonferroni's post hoc analysis was used to assess inter-group differences.

† Determined based on the more severely affected sector.

Table 3. Comparison of the LCD and LCCI Between Affected and Unaffected Sectors of Single Hemi-ONH Damaged Eyes in the Three Groups

Variables	NAION (n = 16)	NTG (n = 22)	Healthy (n = 48)
Superior sector:inferior sector	13:3	18:4	44:4
LCD (μm)			
Affected sector	417.6 ± 83.0	498.8 ± 105.3	443.5 ± 93.2
Unaffected sector	405.2 ± 90.39	477.5 ± 120.2	406.8 ± 93.2
P^*	0.600	0.098	**<0.001**
LCCI			
Affected sector	6.87 ± 1.55	9.76 ± 2.19	6.90 ± 1.35
Unaffected sector	6.84 ± 1.37	8.29 ± 2.25	6.84 ± 1.11
P^*	1.000	**0.010**	0.745

Data are presented as mean ± SD. Factors with statistical significance are shown in bold. For the NAION and NTG groups, eyes with only one hemi-ONH disease were included. For healthy subjects, the comparison was made between the sectors matched for the affected and unaffected sectors of NAION and NTG patients.

* Comparisons were made using Wilcoxon signed-rank tests for NAION and NTG and paired t-tests for healthy subjects.

LC deformation is an important pathophysiologic manifestation of glaucoma even when accompanied by low IOP. The present study assessed LC morphology by measuring LCD and the LCCI, showing that both parameters were significantly larger in NTG than in NAION, despite of similar axonal damage.

Consistent with previous studies,[11,12] LC deformation as assessed by LCD was greater in NTG than in NAION in the present study; however, LCD is measured from the level of the BMO and therefore can be affected by choroidal thickness, which has considerable inter-individual[14] and intra-individual regional variabilities,[15,38] even in normal populations. The LC is a sieve-like perforation in the posterior part of the sclera that is sustained by load-bearing connective tissues of the peripapillary sclera. Because the choroid is therefore unassociated with anteroposterior LC deformation, including choroidal thickness in LCD would lead to a biased assessment of LC morphology.[30] Moreover, the choroid was shown to be thicker in eyes with NAION than in healthy eyes,[13] which may increase LCD in eyes with NAION.

In contrast, the LCCI is less affected by choroidal thickness, suggesting that it may better represent LC deformation than does LCD. Because the LCCI was superior to LCD in predicting glaucoma progression in eyes with suspected glaucoma[28] and open-angle glaucoma,[24] the LCCI may be a better marker of glaucomatous LC deformation. The finding of the present study, that the difference between affected and unaffected sectors in NTG was more distinct with the LCCI than with LCD, suggests that the LCCI is a more useful biomarker than LCD in diagnosing glaucoma. In this context, it is also of note that LCD is larger superiorly than inferiorly, which may be due to thicker peripapillary choroid

Investigative Ophthalmology & Visual Science

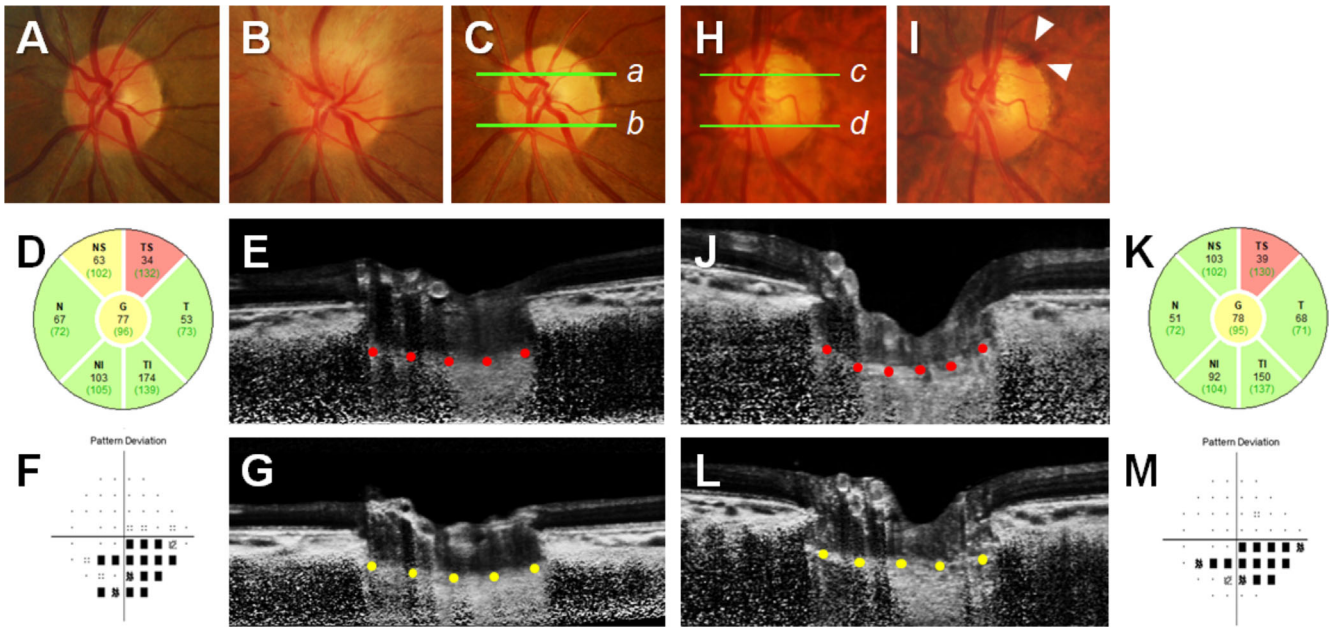

Figure 3. LC morphology of the affected and unaffected hemisectors in eyes with NAION (**A–G**) and NTG (**H–M**). *Green lines* in color disc photographs (**C**, *a*, *b*; **H**, *c*, *d*) indicate the locations of the B-scan images shown in (**E**), (**G**), (**J**), and (**L**), respectively. The *white dotted lines* indicate BMO reference lines (**E** and **J**), and the *red* and *yellow glyphs* indicate the anterior LC surfaces at affected sectors (**E** and **J**) and unaffected sectors (**G** and **L**), respectively. (**A–C**) Disc photographs of a 64-year-old woman with NAION (IOP, 10 mm Hg), taken before she developed NAION (**A**), during the acute phase of NAION (**B**), and after resolution of optic disc edema and the development of optic disc pallor in the superotemporal (ST) sector (**C**, **D**). OCT circular diagram shows RNFL thinning in the superior sector, corresponding to the location of the VF defect (**F**). Comparable LCD and LCCI in the (**E**) affected sectors (*red glyphs*) and (**G**) unaffected sectors (*yellow glyphs*). (**H**, **I**) Disc photographs of a 65-year-old woman with NTG (IOP, 10 mm Hg) and a history of optic disc hemorrhage in the ST sector (*white arrowheads,* **I**). Glaucomatous damage is noted in the superior sector by the OCT circular diagram (**K**), and the VF pattern deviation plot shows corresponding VF defects (**M**). Note that LCD (*double-headed arrows*) and the LCCI (*red glyphs*) were larger in the affected hemisector of the eye with NTG (**J**) than in the corresponding sector of the eye with NAION (**E**). Regional difference in LCCI between affected sectors (*red glyphs*, **J**) and unaffected sectors (*yellow glyphs*, **L**), corresponding to the location of RNFL damage, is also notable in the NTG eye.

in the superior region,[39] whereas the LCCI is symmetrically distributed in the superior and inferior regions (Fig. 2).

Consistent with our previous findings,[25] the present study showed that LCCI was significantly larger in the affected than in the unaffected sector of NTG eyes with damage to a single hemi-ONH. This regional difference, however, was not observed in eyes with NAION. Because RNFL thicknesses in both the affected and unaffected sectors were similar in both groups of eyes, axonal damage alone was unlikely to be a causative factor of the larger LCCI in NTG eyes. This finding also indicates that the mechanisms of axonal loss differ between NTG and NAION, with deformed LC being more suggestive of GON.

Caution is needed, however, in using LC configuration to distinguish between NAION and NTG. Because NTG is a multifactorial disease that is not solely explained by mechanical stress, some NTG patients with lower systemic blood pressure or large parapapillary atrophy may tend to have a smaller LCCI.[29] In addition, inter-individual variability in LC configuration can result in the LCCI being comparable in some NTG eyes and healthy eyes.[29] Under these conditions, fundus examination for disc pallor, excavation, or cupping; evaluation of prelaminar tissue thickness[11] and configuration[40]; and a clinical history of changes in a patient's vision may help in the differential diagnosis. Recent studies using OCT angiography showed that peripapillary[41,42] and macular[42] microvasculature may also differ between NAION and open-angle glaucoma, under similar degrees of visual field damage. Although findings are controversial between the studies,[41,42] OCT angiography could be another tool for distinguishing between NAION and GON, together with assessment of the LC morphology.

The present study had several limitations. First, this study included a relatively small number of subjects, all of whom were Korean; therefore, these results may not be directly applicable to patients of other ethnicities. Second, only the LC within the BMO was included in the measurement of LC curvatures, as the LC was often not visible outside this region due to the shadowing effect of the choroid. However, the LCCI measured from the entire LC (i.e., between the LC insertions) was comparable to that measured on the LC within the BMO in our previous study,[27] indicating that the curvature of the LC assessed within the BMO may be a surrogate measurement of actual LC curvature. In addition, we showed that the LCCI was useful not only in diagnosing early glaucoma[30] but also in predicting the development[28] and progression of glaucoma.[24] Third, LC thicknesses were not compared in the present study due to the difficulty of detecting the posterior border of the LC in some NAION and healthy eyes. Finally, given the strict criteria for inclusion in each diagnostic group, the results of our study may not be directly applied to eyes with conditions such as a tilted or torted disc.

In conclusion, LC morphology differed between eyes with NAION and NTG, despite their similar degree of IOP and RNFL damage. Evaluation of LC morphology may help us understand the distinctive pathophysiology of NAION, which differs from that of NTG.

Acknowledgments

Supported by a grant from the Seoul National University Bundang Hospital Research Fund (02-2017-037). The abstract of this article was awarded a travel grant by ARVO in 2020. The funder had no role in the design or conduct of this research.

Disclosure: **J.-A. Kim**, None; **E.J. Lee**, None; **T.-W. Kim**, None; **H. Kim**, None; **M.J.A. Girard**, None; **J.M. Mari**, None; **H.K. Yang**, None; **J.-M. Hwang**, None

References

1. Hayreh SS. Ischemic optic neuropathy. *Prog Retin Eye Res*. 2009;28:34–62.
2. Pasol J. Neuro-ophthalmic disease and optical coherence tomography: glaucoma look-alikes. *Curr Opin Ophthalmol*. 2011;22:124–132.
3. Hayreh SS, Zimmerman B. Visual field abnormalities in nonarteritic anterior ischemic optic neuropathy: their pattern and prevalence at initial examination. *Arch Ophthalmol*. 2005;123:1554–1562.
4. Colen TP, van Everdingen JA, Lemij HG. Axonal loss in a patient with anterior ischemic optic neuropathy as measured with scanning laser polarimetry. *Am J Ophthalmol*. 2000;130:847–850.
5. Hayreh SS, Zimmerman MB. Incipient nonarteritic anterior ischemic optic neuropathy. *Ophthalmology*. 2007;114:1763–1772.
6. Burgoyne CF, Downs JC, Bellezza AJ, Suh JK, Hart RT. The optic nerve head as a biomechanical structure: a new paradigm for understanding the role of IOP-related stress and strain in the pathophysiology of glaucomatous optic nerve head damage. *Prog Retin Eye Res*. 2005;24:39–73.
7. Bellezza AJ, Rintalan CJ, Thompson HW, Downs JC, Hart RT, Burgoyne CF. Deformation of the lamina cribrosa and anterior scleral canal wall in early experimental glaucoma. *Invest Ophthalmol Vis Sci*. 2003;44:623–637.
8. Yang H, Ren R, Lockwood H, et al. The connective tissue components of optic nerve head cupping in monkey experimental glaucoma Part 1: global change. *Invest Ophthalmol Vis Sci*. 2015;56:7661–7678.
9. Yang H, Williams G, Downs JC, et al. Posterior (outward) migration of the lamina cribrosa and early cupping in monkey experimental glaucoma. *Invest Ophthalmol Vis Sci*. 2011;52:7109–7121.
10. Kim JA, Kim TW, Lee EJ, Kim JM, Girard MJA, Mari JM. Intereye comparison of lamina cribrosa curvature in normal tension glaucoma patients with unilateral damage. *Invest Ophthalmol Vis Sci*. 2019;60:2423–2430.
11. Lee EJ, Choi YJ, Kim TW, Hwang JM. Comparison of the deep optic nerve head structure between normal-tension glaucoma and nonarteritic anterior ischemic optic neuropathy. *PLoS One*. 2016;11:e0150242.
12. Fard MA, Afzali M, Abdi P, et al. Optic nerve head morphology in nonarteritic anterior ischemic optic neuropathy compared to open-angle glaucoma. *Invest Ophthalmol Vis Sci*. 2016;57:4632–4640.
13. Fard MA, Abdi P, Kasaei A, Soltani Mogaddam R, Afzali M, Moghimi S. Peripapillary choroidal thickness in nonarteritic anterior ischemic optic neuropathy. *Invest Ophthalmol Vis Sci*. 2015;56:3027–3033.
14. Rhodes LA, Huisingh C, Johnstone J, et al. Peripapillary choroidal thickness variation with age and race in normal eyes. *Invest Ophthalmol Vis Sci*. 2015;56:1872–1879.
15. Johnstone J, Fazio M, Rojananuangnit K, et al. Variation of the axial location of Bruch's membrane opening with age, choroidal thickness, and race. *Invest Ophthalmol Vis Sci*. 2014;55:2004–2009.
16. Jonas JB, Papastathopoulos KI. Optic disc shape in glaucoma. *Graefes Arch Clin Exp Ophthalmol*. 1996;234(suppl 1):S167–173.
17. Vongphanit J, Mitchell P, Wang JJ. Population prevalence of tilted optic disks and the relationship of this sign to refractive error. *Am J Ophthalmol*. 2002;133:679–685.
18. Samarawickrama C, Mitchell P, Tong L, et al. Myopia-related optic disc and retinal changes in adolescent children from Singapore. *Ophthalmology*. 2011;118:2050–2057.
19. Lee EJ, Kim TW, Weinreb RN, Park KH, Kim SH, Kim DM. Visualization of the lamina cribrosa using enhanced depth imaging spectral-domain optical coherence tomography. *Am J Ophthalmol*. 2011;152:87–e81.
20. Girard MJ, Strouthidis NG, Ethier CR, Mari JM. Shadow removal and contrast enhancement in optical coherence tomography images of the human optic nerve head. *Invest Ophthalmol Vis Sci*. 2011;52:7738–7748.
21. Girard MJ, Tun TA, Husain R, et al. Lamina cribrosa visibility using optical coherence tomography: comparison of devices and effects of image enhancement techniques. *Invest Ophthalmol Vis Sci*. 2015;56:865–874.
22. Mari JM, Strouthidis NG, Park SC, Girard MJ. Enhancement of lamina cribrosa visibility in optical coherence tomography images using adaptive compensation. *Invest Ophthalmol Vis Sci*. 2013;54:2238–2247.
23. Park SC, Kiumehr S, Teng CC, Tello C, Liebmann JM, Ritch R. Horizontal central ridge of the lamina cribrosa and regional differences in laminar insertion in healthy subjects. *Invest Ophthalmol Vis Sci*. 2012;53:1610–1616.
24. Lee EJ, Kim TW, Kim H, Lee SH, Girard MJ, Mari JM. Comparison between lamina cribrosa depth and curvature as a predictor of progressive retinal nerve fiber layer thinning in primary open-angle glaucoma. *Ophthalmol Glaucoma*. 2018;1:44–51.
25. Kim JA, Kim TW, Lee EJ, Girard MJA, Mari JM. Lamina cribrosa morphology in glaucomatous eyes with hemifield defect in a Korean population. *Ophthalmology*. 2019;126:692–701.
26. Lee SH, Kim TW, Lee EJ, Girard MJA, Mari JM. Lamina cribrosa curvature in healthy Korean eyes. *Sci Rep*. 2019;9:1756.
27. Lee SH, Yu DA, Kim TW, Lee EJ, Girard MJ, Mari JM. Reduction of the lamina cribrosa curvature after trabeculectomy in glaucoma. *Invest Ophthalmol Vis Sci*. 2016;57:5006–5014.
28. Kim JA, Kim TW, Weinreb RN, Lee EJ, Girard MJA, Mari JM. Lamina cribrosa morphology predicts progressive retinal nerve fiber layer loss in eyes with suspected glaucoma. *Sci Rep*. 2018;8:738.
29. Lee SH, Kim TW, Lee EJ, Girard MJA, Mari JM, Ritch R. Ocular and clinical characteristics associated with the extent of posterior lamina cribrosa curve in normal tension glaucoma. *Sci Rep*. 2018;8:961.
30. Lee SH, Kim TW, Lee EJ, Girard MJ, Mari JM. Diagnostic power of lamina cribrosa depth and curvature in glaucoma. *Invest Ophthalmol Vis Sci*. 2017;58:755–762.
31. Lee EJ, Kim TW, Kim M, Girard MJ, Mari JM, Weinreb RN. Recent structural alteration of the peripheral lamina cribrosa near the location of disc hemorrhage in glaucoma. *Invest Ophthalmol Vis Sci*. 2014;55:2805–2815.
32. Kiumehr S, Park SC, Syril D, et al. In vivo evaluation of focal lamina cribrosa defects in glaucoma. *Arch Ophthalmol*. 2012;130:552–559.
33. Olver JM, Spalton DJ, McCartney AC. Microvascular study of the retrolaminar optic nerve in man: the possible significance in anterior ischaemic optic neuropathy. *Eye (Lond)*. 1990;4:7–24.

Investigative Ophthalmology & Visual Science

34. Jonas JB, Berenshtein E, Holbach L. Anatomic relationship between lamina cribrosa, intraocular space, and cerebrospinal fluid space. *Invest Ophthalmol Vis Sci*. 2003;44:5189–5195.
35. Anderson DR, Hendrickson A. Effect of intraocular pressure on rapid axoplasmic transport in monkey optic nerve. *Invest Ophthalmol*. 1974;13:771–783.
36. Minckler DS, Bunt AH, Johanson GW. Orthograde and retrograde axoplasmic transport during acute ocular hypertension in the monkey. *Invest Ophthalmol Vis Sci*. 1977;16:426–441.
37. Hernandez MR. The optic nerve head in glaucoma: role of astrocytes in tissue remodeling. *Prog Retin Eye Res*. 2000;19:297–321.
38. Rhodes LA, Huisingh C, Johnstone J, et al. Variation of laminar depth in normal eyes with age and race. *Invest Ophthalmol Vis Sci*. 2014;55:8123–8133.
39. Jiang R, Wang YX, Wei WB, Xu L, Jonas JB. Peripapillary choroidal thickness in adult Chinese: the Beijing Eye Study. *Invest Ophthalmol Vis Sci*. 2015;56:4045–4052.
40. Lee EJ, Han JC, Park DY, Kee C. Difference in topographic pattern of prelaminar and neuroretinal rim thinning between nonarteritic anterior ischemic optic neuropathy and glaucoma. *Invest Ophthalmol Vis Sci*. 2019;60:2461–2467.
41. Mastropasqua R, Agnifili L, Borrelli E, et al. Optical coherence tomography angiography of the peripapillary retina in normal-tension glaucoma and chronic nonarteritic anterior ischemic optic neuropathy. *Curr Eye Res*. 2018;43:778–784.
42. Liu CH, Wu WC, Sun MH, Kao LY, Lee YS, Chen HS. Comparison of the retinal microvascular density between open angle glaucoma and nonarteritic anterior ischemic optic neuropathy. *Invest Ophthalmol Vis Sci*. 2017;58:3350–3356.